

Chapter 45

On the Behaviour of Structures with Many Nonlinear Elements

T. Rogers, G. Manson, and K. Worden

Abstract One of the most powerful methods currently available for the analysis of structural dynamics at high frequencies is Statistical Energy Analysis (SEA). The fundamental idea behind the method is that, at higher frequencies, so many modes are present in the response of the structure that individual modes cease to be resolvable and a simplified statistical order emerges in the response. Although the details of the context are very different to SEA, the current paper is motivated by it and provides a preliminary investigation into what happens when very many nonlinear elements are present in a structure under random vibration; the question being, does a simplified statistical order emerge as the influence of the nonlinearities increases? A number of case studies are provided based on computer simulation, arguing the case that order does indeed appear to emerge and a parallel with the SEA case is thus drawn.

Keywords Nonlinear structural dynamics • Random vibration • Emergent properties • Effective models

45.1 Introduction

As the use of numerical modelling techniques, such as Finite Element Analysis (FEA), becomes more commonplace as a key part of the design process, as opposed to physical testing, the requirement for reliability of the results produced increases. This is especially the case for high-value structures such as aircraft, bridges and offshore structures. This is not simply a matter of going to ever-increasingly complex models in the hope of modelling ever more detailed behaviour; it is also a matter of understanding the uncertainties inherent in the modelling process and quantifying the resulting uncertainty in predictions. These issues are particularly felt in the case of nonlinear structures and systems because of the very different types of behaviour they can exhibit. The understanding of nonlinear dynamic behaviour, therefore, is vital for producing reliable model predictions, from detailed time series behaviour to fatigue life estimates. Because even systems with very small numbers of degrees of freedom (DoFs) can exhibit complex behaviour, the focus of much academic research up to this point has been in understanding the behaviour of simple nonlinear systems with few nonlinearities present in low DoF cases [1].

In contrast to analytical work, the typical FEA model may have a very high number of degrees of freedom present, around which a great number of nonlinear elements could be located. (However, the models used in FEA will typically be used to identify only the lower frequency modes of a structure and, therefore it is usually considered a low frequency method.) For nonlinear systems there is a clear disconnect between what is possible with theoretical methods and what is possible with numerical methods. Another issue in modelling nonlinear systems is associated with the computational cost of calculating natural frequencies for very large system matrices. Even for linear systems, the cost of solving the eigenvalue problems may be high, even with modern approaches [2]; in order to compute nonlinear responses using FEA, explicit time step solvers are used for which the computational cost is extremely high. For linear FEA, one option is to compute reduced order models, and there are many techniques which can be considered reliable [3]; the situation is not so well-developed in the case of nonlinear models. There remains a great deal of work to be done on the general problem of understanding and modelling nonlinear systems with many DoFs and there remains a gulf between what can be modelled and what can be analysed mathematically.

One possibility that may allow analytical progress is that nonlinear systems with many DoFs and nonlinear elements may allow the use of *effective models* with low numbers of DoFs which are obtained by system identification or learning from data. The term ‘effective model’ is borrowed from theoretical particle physics where it is used to denote a model which does not encompass all of the detailed physics, but can nonetheless make predictions in certain regimes of energy.

T. Rogers • G. Manson • K. Worden (✉)

Dynamics Research Group, Department of Mechanical Engineering, University of Sheffield, Mappin Street, Sheffield S1 3JD, UK
e-mail: k.worden@sheffield.ac.uk

The analogy explored in this paper is a simplified effective model for nonlinear systems which might make predictions at certain levels of excitation. This analogy was motivated by test results communicated to the authors based on a modal test of a helicopter structure. When the structure was tested on the ground, the low-frequency response was dominated by clear modes as expected; however, the structure was revealed to be nonlinear because the resonance frequencies shifted when the level of excitation was increased. Somewhat surprisingly, when the structure was tested in flight at much higher levels of excitation, the modal structure disappeared and an almost flat power spectrum was obtained. Although the context is very different, the authors were reminded of the situation where Statistical Energy Analysis (SEA) applies. SEA can be used at high frequencies where the high modal densities render individual modes indistinguishable and a statistical order emerges which allows a much simplified analysis based on power flow between substructures [4, 5]. This observation led to the hypothesis considered in this paper, that a system with many nonlinearities may have a simplified response at levels of forcing where the nonlinearities are all fully excited. To stretch the analogy with SEA somewhat, the idea was to investigate if a sort of statistical order can emerge. To be perfectly clear, there is no intention here to propose a nonlinear theory of SEA; that is an entirely different problem which is being pursued effectively elsewhere [6].

The layout of the paper is as follows: in Sect. 45.2, the methods of numerical simulation used in the paper are discussed and benchmarked. In Sect. 45.3, the developed solver is used to simulate the behaviour of multi-DoF systems with many nonlinear elements. The paper is finalised with a short conclusions section.

45.2 Framework for Simulation

Although the methods used could apply to many different types of nonlinearity it was chosen that this investigation would focus on systems whose equations of motion take the form,

$$[m]\{\ddot{y}\} + [c]\{\dot{y}\} + [k]\{y\} + \{f(\{y\})\} = \{x(t)\} \quad (45.1)$$

i.e. the standard linear second order system with stiffness nonlinearities. To further simplify matters, only hardening cubic stiffness nonlinearities were included between DoFs via the vector $\{f(\{y\})\}$. In order to allow the inclusion of many nonlinear springs, a solver was constructed in Matlab [7] which could integrate systems of equations with moderate numbers of DoFs i.e. up to a few hundred. A number of different methods were assessed for solving the initial value problem, these included both fixed step and adaptive methods. Since the system response was to be measured against a simulated Gaussian white noise input, a fixed step method was adopted; This was due to the adaptive methods sometimes becoming ‘stuck’ when trying to take account of the large gradients in the random forcing. The integration method used was a 5th order Runge-Kutta method-Butcher’s Method [8]. Because the algorithm is not so common, the update equations are given here,

$$\begin{aligned} y_{i+1} &= \frac{1}{90} (7k_1 + 32k_3 + 12k_4 + 32k_5 + 7k_6) h \\ k_1 &= f(t_i, y_i) \\ k_2 &= f\left(t_i + \frac{1}{4}h, y_i + \frac{1}{4}k_1h\right) \\ k_3 &= f\left(t_i + \frac{1}{4}h, y_i + \frac{1}{8}k_1h + \frac{1}{8}k_2h\right) \\ k_4 &= f\left(t_i + \frac{1}{2}h, y_i - \frac{1}{2}k_2h + k_3h\right) \\ k_5 &= f\left(t_i + \frac{3}{4}h, y_i + \frac{3}{16}k_1h + \frac{9}{16}k_4h\right) \\ k_6 &= f\left(t_i + h, y_i - \frac{3}{7}k_1h + \frac{2}{7}k_2h + \frac{12}{7}k_3h - \frac{12}{7}k_4h + \frac{8}{7}k_5h\right) \end{aligned} \quad (45.2)$$

where the vector braces for the iterates y_i have been suppressed and it should be understood that the equations have motion have been cast in first-order form; the timestep is denoted h . For all the simulations run here, the initial conditions adopted were $\{y\} = \{\dot{y}\} = \{0\}$. A sampling frequency of 10 kHz was adopted throughout, yielding a timestep of 0.1 ms. All Frequency

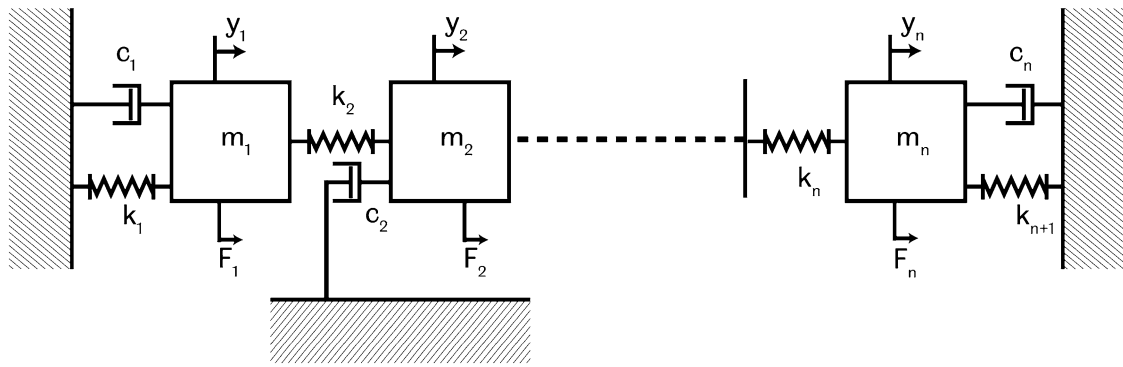


Fig. 45.1 n -DoF linear chain system which forms the basis for the analysis

Response Function (FRF) plots were generated by running 200 parallel simulations each for 100 s at 10 kHz with a different realisation of the random forcing. The FRF of each of the 200 time domain signals was computed after discarding the first 10 s of time domain data to remove transient behaviour. The FRF values were then averaged across the 200 realisations.

As a basis for investigating the effect of nonlinearities on high DoF systems, first a linear chain system (Fig. 45.1) was generated with a unit mass matrix, tri-diagonal stiffness matrix and damping matrix proportional to the mass matrix. All springs were set to have stiffness coefficient $k_i = k = 10^4 \text{ N m}^{-1}$, damping coefficients were all set to $c_i = c = 5 \text{ N s m}^{-1}$ and masses $m_i = m = 1 \text{ kg}$. This prescription gives a damping ratio $\zeta = 0.025$ for an SDoF system which is 2.5 % of critical damping. The system matrices are thus $[m] = [I]$, $[c] = 5 \times [I]$ (where $[I]$ is the identity matrix) and $[k]$ is a tridiagonal matrix with the diagonal values equal to $2k$ and the off diagonal non-zero elements equal to $-k$. The linear system is well understood and its natural frequencies, mode shapes and frequency response can be computed straightforwardly.

The integration method was checked, initially, by numerically generating FRFs for known linear systems and comparing them with analytical predictions. First, a low DoF system was considered. For a three DoF system, generated with the parameters described previously, the numerical and theoretical results can be seen to be in excellent agreement for both the magnitude and phase components of the FRF (Fig. 45.2). When the number of simulated DoFs was increased to 30, the same agreement could be seen (Fig. 45.3).

The next benchmark assessed the ability of the modeller to handle nonlinear equations of motion. For this exercise, the chain system with three degrees of freedom was considered. A single cubic spring was added as discussed in [9]; for this system, the effect of the position of the cubic spring can be classified in three ways. System Type A is an asymmetric system, obtained when the nonlinearity is placed between mass one and ground, mass three and ground, mass one and two or mass two and three. In this case all modes will exhibit nonlinear behaviour. System Type B occurs when the nonlinear spring is between mass two and ground; in this case mode two is linear since mass two remains stationary in that mode. Type C is obtained if the nonlinear spring connects masses one and three; in this case modes one and three remain linear since masses one and three move in phase in these modes. The simulation results for these systems can be seen in Fig. 45.4. A further set of simulations considered the effects of harmonic forcing at 4 Hz on the systems with a single DoF or 30 DoF; the linear systems and those with a single cubic spring connecting mass one to ground were considered. When spectra were computed for the responses (Figs. 45.5–45.8), the expected variation in harmonic content with level of excitation was observed. This exercise concluded the benchmarking of the numerical solver.

45.3 Effect of Nonlinear Elements

With the conviction that the numerical modeller accurately represents the motion of the systems of interest, a routine was developed to investigate the effect of cubic nonlinearities being introduced into the system in multiple random locations. This allowed the number of nonlinearities in the system to be controlled by automatically generating a matrix with a given number of nonlinear springs equal in size to the linear stiffness matrix. The first set of investigations considered the effect of inserting a single cubic spring into the linear chain system.

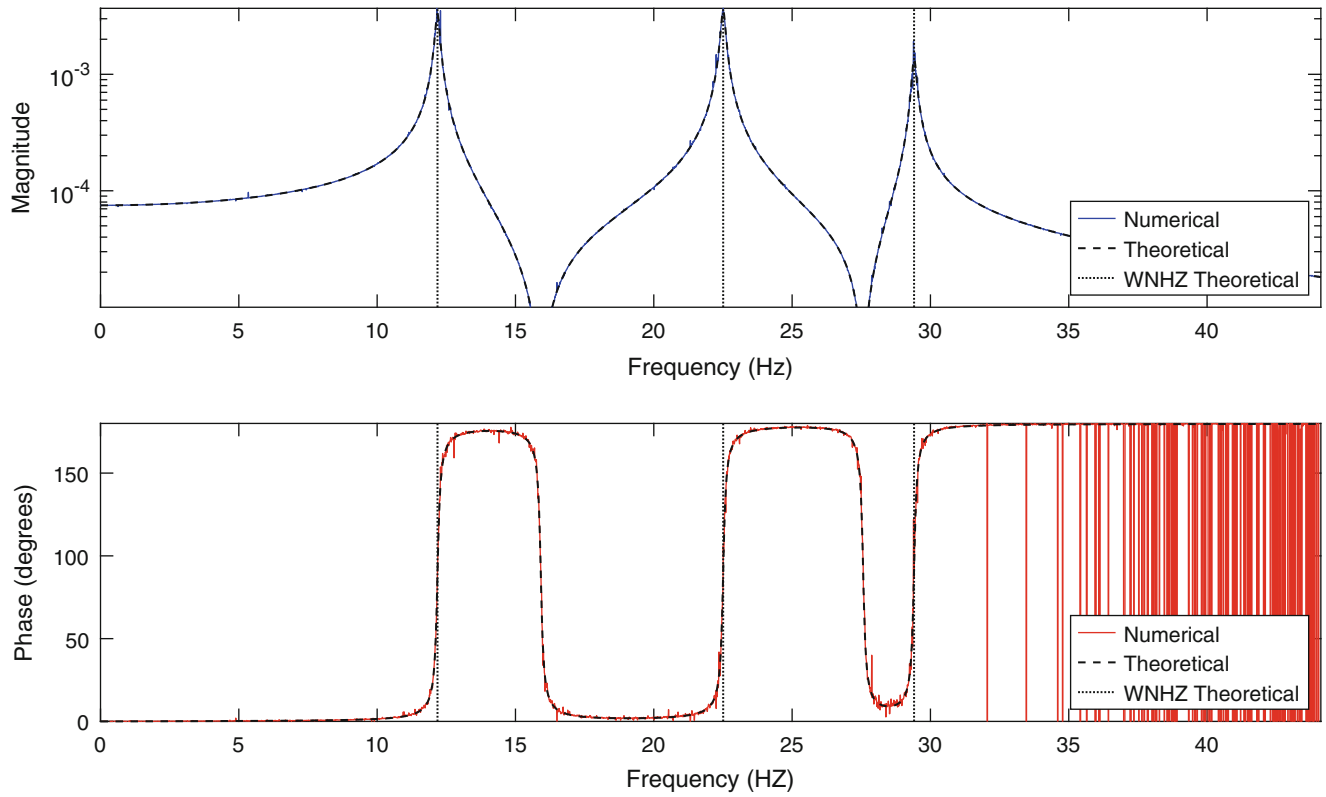


Fig. 45.2 Theoretical and numerical FRFs for 3DoF benchmark system. Vertical lines indicate the natural frequencies (WNHZ Theoretical)

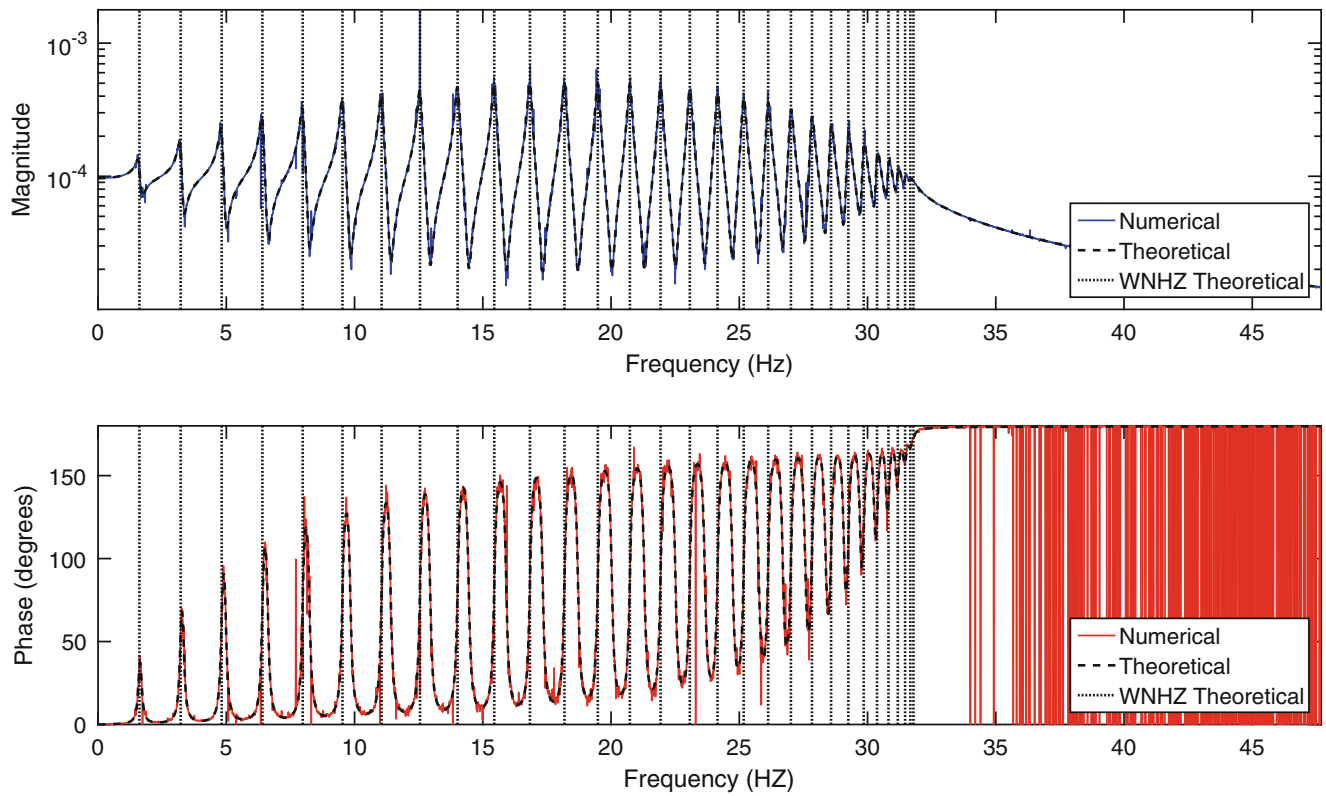


Fig. 45.3 Theoretical and numerical FRFs for 30DoF benchmark system. Vertical lines indicate the natural frequencies (WNHZ Theoretical)

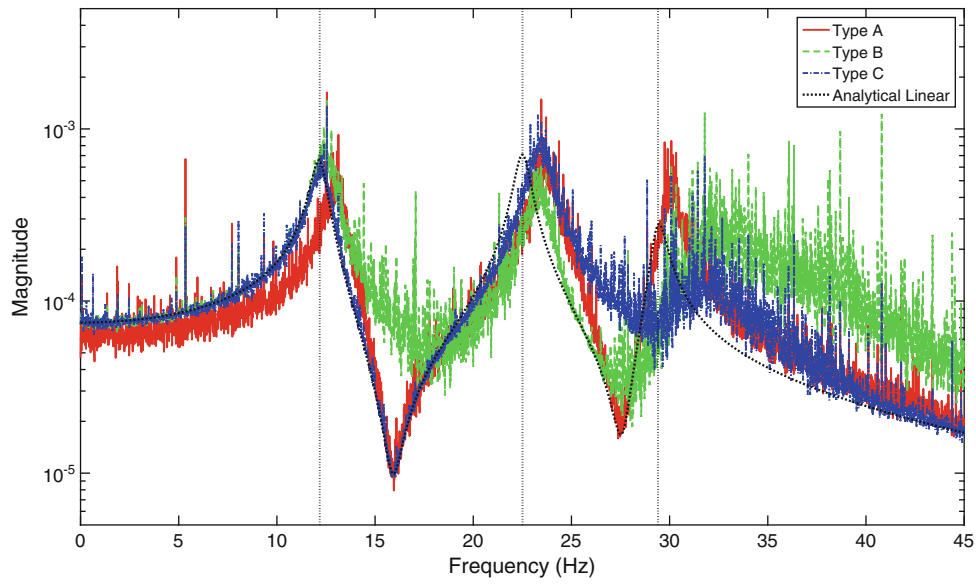


Fig. 45.4 Figure showing comparison of FRFs produced for three characteristic types of nonlinear 3DOF system

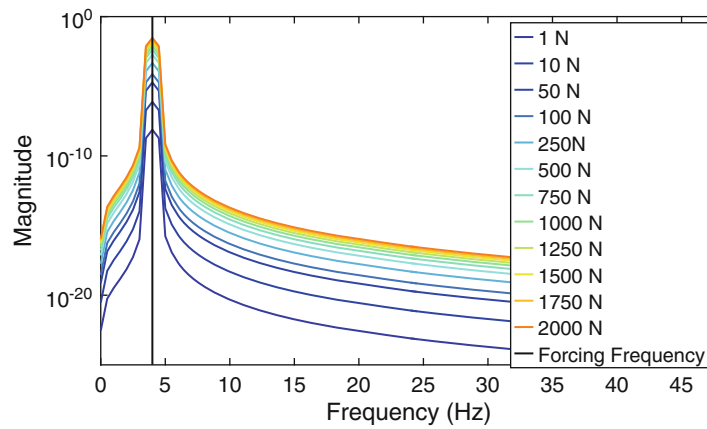


Fig. 45.5 Response of a SDOF linear system to varying magnitude 4 Hz sine wave input

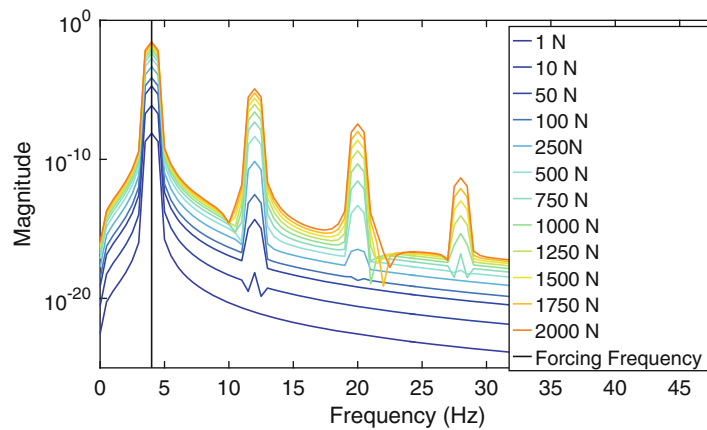


Fig. 45.6 Response of a SDOF system with a cubic nonlinearity at mass 1 to varying magnitude 4 Hz sine wave input

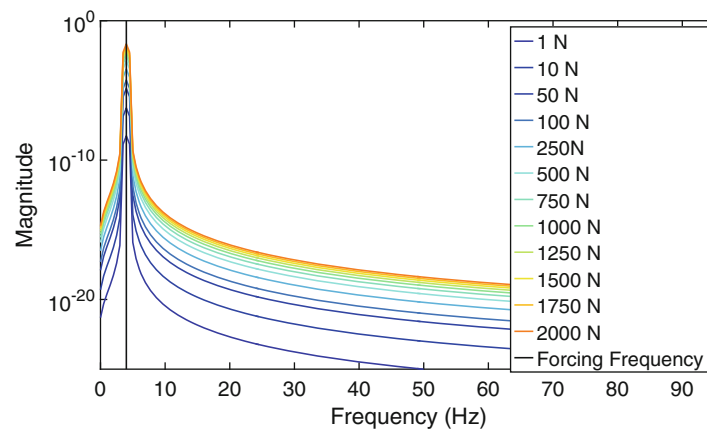


Fig. 45.7 Response of a 30DOF linear system to varying magnitude 4 Hz sine wave input

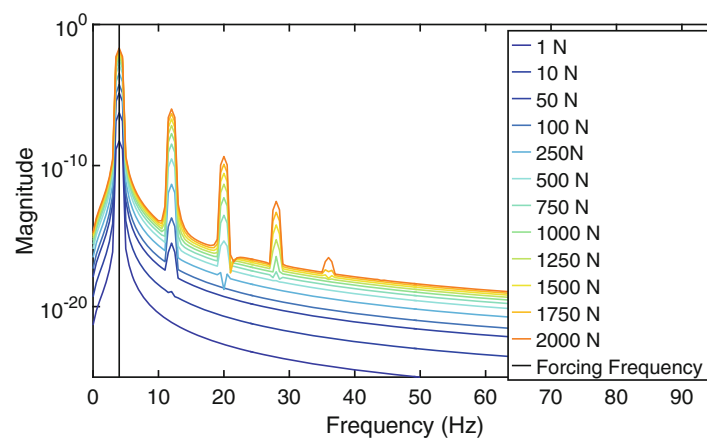


Fig. 45.8 Response of a 30DOF system with a cubic nonlinearity at mass 1 to varying magnitude 4 Hz sine wave input

45.3.1 Single Element Location

Three tests were run with a single nonlinearity randomly placed in the system. The nonlinear springs respectively connected masses 7 and 26, 1 and 6 and 22 and 26 in each of the three tests. The nonlinear coefficient k_3 of these springs was initially set to a constant value at 10^4 N m^{-3} . First of all, the responses were obtained with an increasing magnitude of Gaussian white noise forcing. For the first position, the effect of the nonlinearity can be seen as the forcing is increased (Fig. 45.9); the linear modal structure seen at low forcing is clearly disrupted by the presence of the nonlinear spring between masses seven and 26. Even at very high magnitude there is still a clear modal structure; many distinct peaks can be clearly seen.

The results for the other two positions are shown in Figs. 45.10 and 45.11. It is clear that even when there is only a single nonlinearity in the system, the location of that nonlinearity has a large effect on the system response. This makes sense; if a nonlinear spring connects two masses that move in phase for many of the modes, there will be less overall distortion, even with very high forcing. If the nonlinear spring connects two masses that have low relative displacement in many of the modes there will be minimal distortion at lower excitations, but with increased excitation the nonlinear behaviour will become evident.

It is also clear that the presence of a single nonlinear element in a system with many DoFs is inadequate to mask or ‘wash out’ the modal structure as was observed in the helicopter test mentioned in the introduction. It was next investigated whether the introduction of many more nonlinear elements to the system would lead to masking of the modal structure; a form of statistical order emerging where the effects of the nonlinearities at many points in the structure would interact leading a simpler FRF.

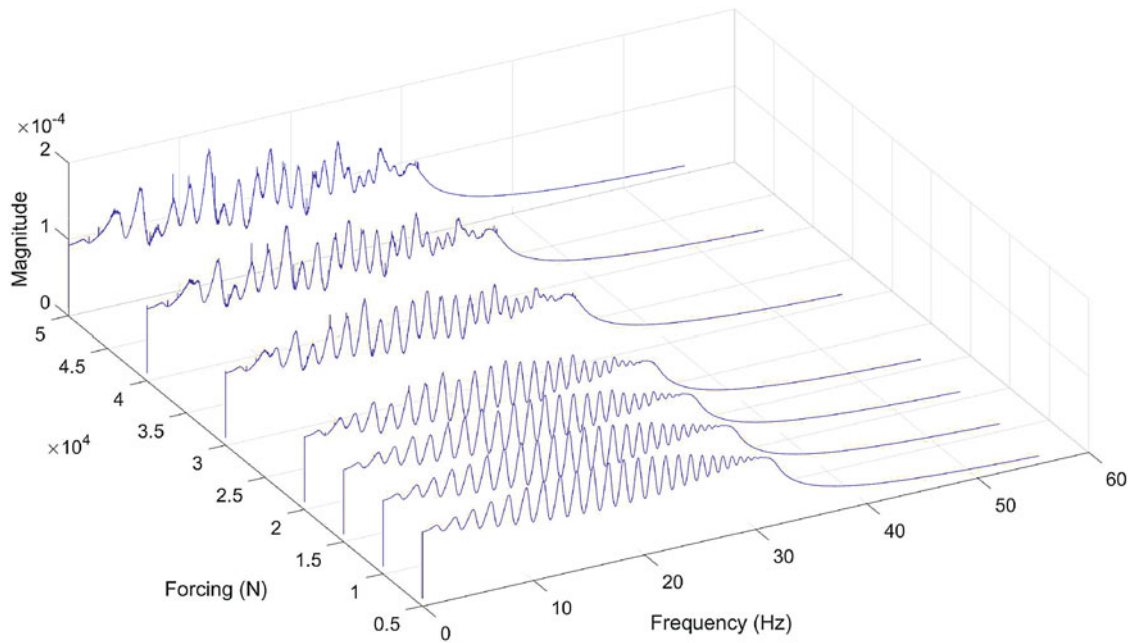


Fig. 45.9 Effect on the FRF of a single cubic spring with coefficient $k_3 = 10^4 \text{ N m}^{-3}$, positioned between masses 7 and 6, for varying magnitude of Gaussian white noise forcing

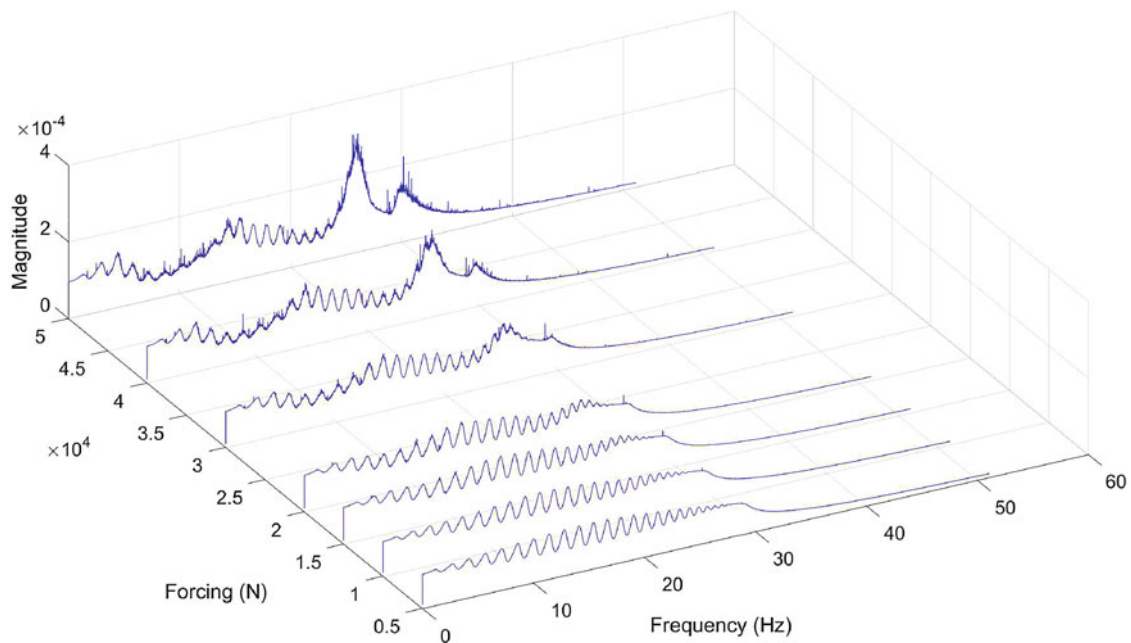


Fig. 45.10 Effect on the FRF of a single cubic spring with coefficient $k_3 = 10^4 \text{ N m}^{-3}$, positioned between masses 1 and 6, for varying magnitude of Gaussian white noise forcing

45.3.2 Multiple Nonlinearities

Simulations were next run by adding randomly distributed nonlinear cubic springs to the underlying linear chain system. Systems containing 30, 50 and 100 nonlinear springs were investigated initially with a variable magnitude forcing and fixed k_3 values; then with fixed forcing and variable k_3 . The results presented here will be for the simulations with increasing k_3 (Figs. 45.12, 45.13, and 45.14).

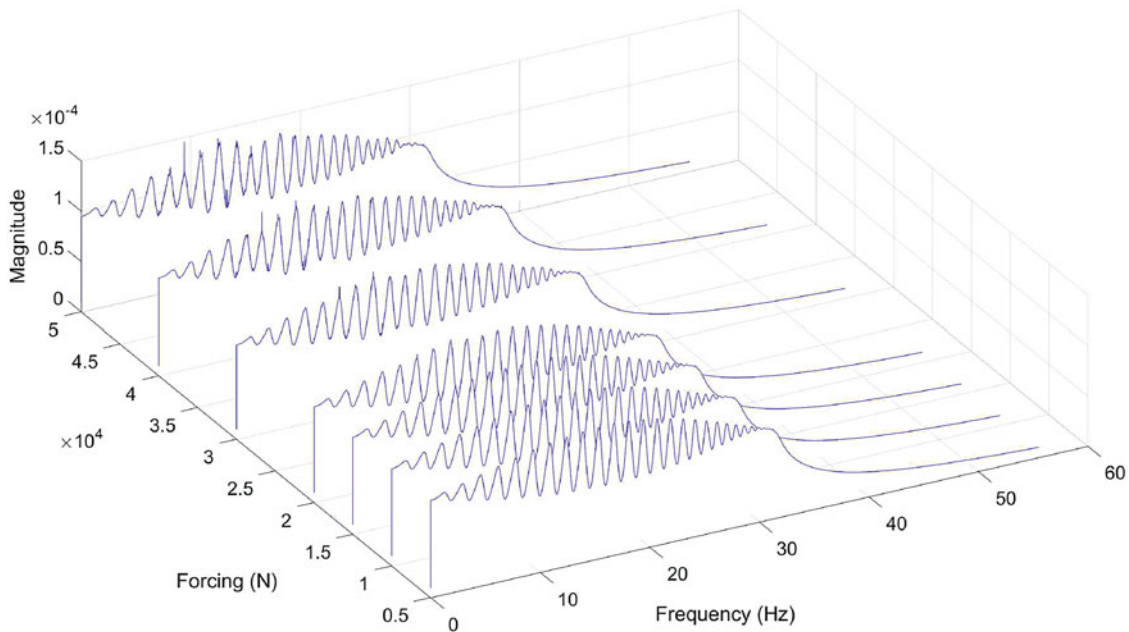


Fig. 45.11 Effect on the FRF of a single cubic spring with coefficient $k_3 = 10^4 \text{ N m}^{-3}$, positioned between masses 22 and 26, for varying magnitude of Gaussian white noise forcing

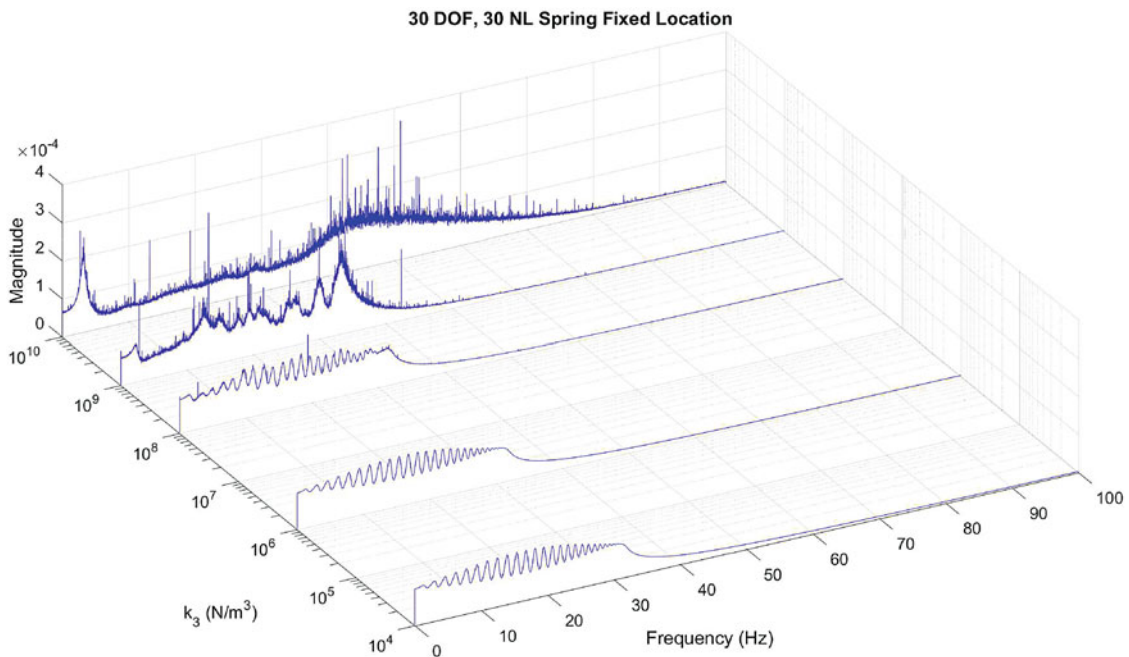


Fig. 45.12 FRF of response at mass 1 for Gaussian random forcing of 100 N on a 30 DoF linear chain system with 30 cubic nonlinearities randomly located in the system. The value of k_3 is increased and the modal structure of the system is clearly removed as the effect of the nonlinearity increases

Considering Fig. 45.12, there is a clear modal structure at low values of k_3 . This structure closely resembles that of the underlying linear system seen in Fig. 45.3; it may be inferred that the presence of the nonlinearities in the system are having little effect on the modal behaviour. With increasing coefficient size, distortion to the linear modal structure becomes apparent by $k_3 = 10^8 \text{ N m}^{-3}$; the effect is a complete disruption of the linear modal structure by $k_3 = 10^9 \text{ N m}^{-3}$ and by $k_3 = 10^{10} \text{ N m}^{-3}$ it has become almost impossible to distinguish more than two ‘resonance’ peaks: one at low frequency and one at high.

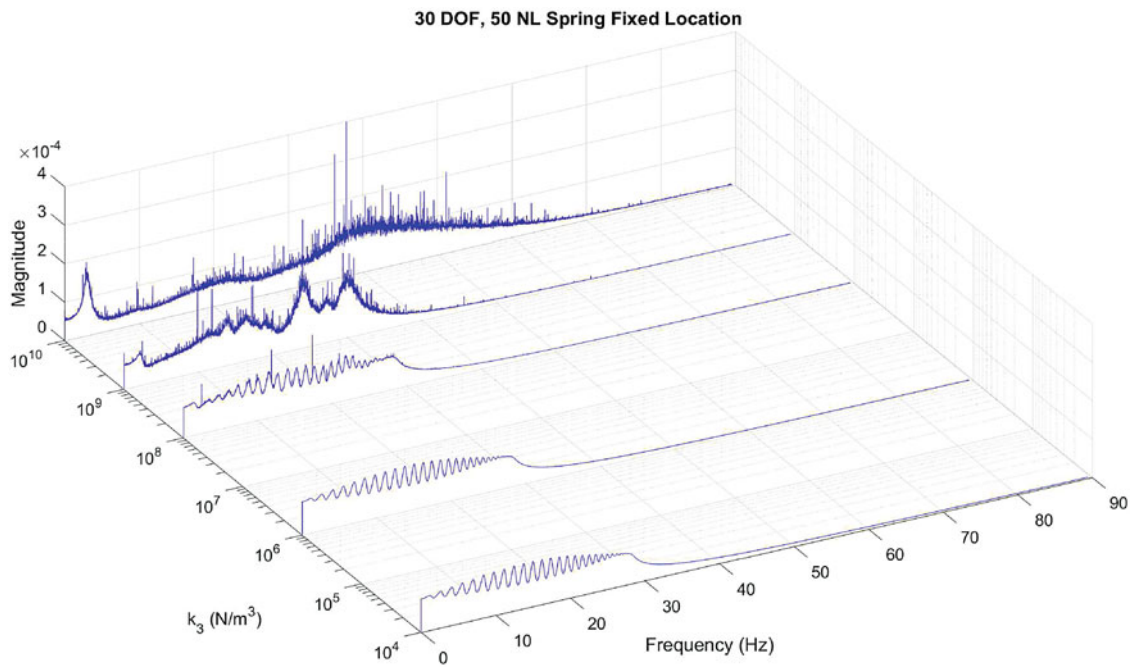


Fig. 45.13 FRF of response at mass 1 for a Gaussian random forcing of 100 N on a 30 DoF linear chain system with 50 cubic nonlinearities randomly located in the system. The value of k_3 is steadily increased as before

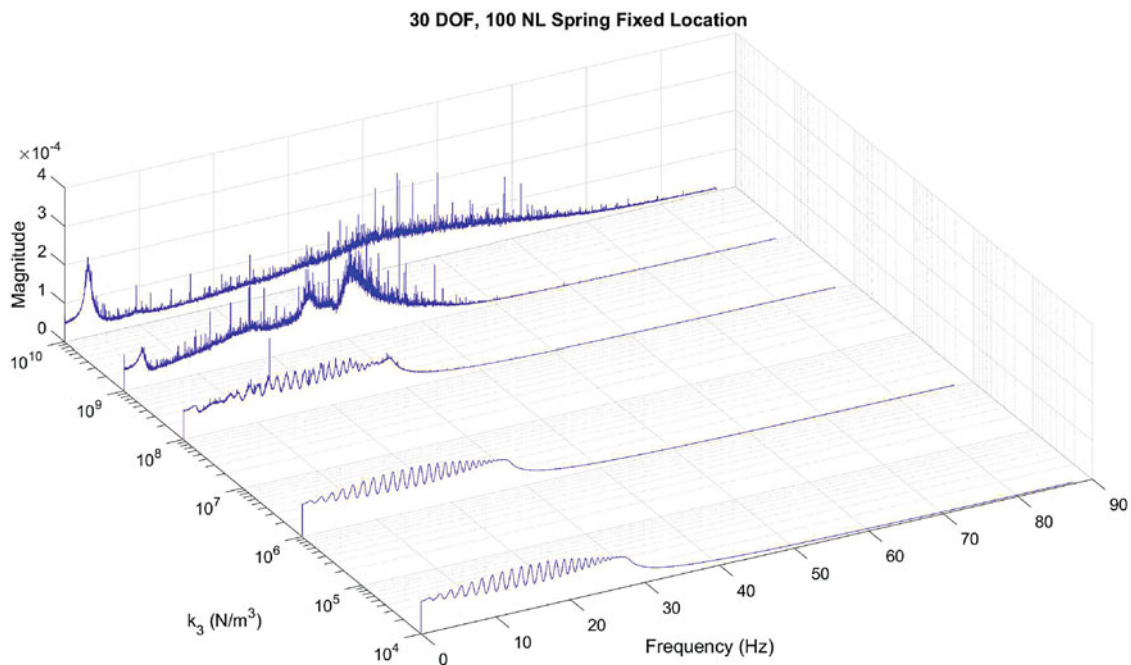


Fig. 45.14 FRF of response at mass 1 for a Gaussian random forcing of 100 N on a 30 DoF linear chain system with 100 cubic nonlinearities randomly located in the system. The value of k_3 is steadily increased as before

It is therefore seen that, as the nonlinear effects in the system increase, the linear modal structure is washed out, with the FRF tending towards only two identifiable peaks. A significant low frequency peak is seen close to the first natural frequency of the linear system and another peak is seen at frequencies significantly above the highest natural frequency of the underlying linear system. It appears that the action of the nonlinearities is to channel energy up and down the spectrum, washing out the linear modal structure, it is this washing out that may allow parallels to be drawn with SEA and opens up the possibility of using average energies to understand response across all frequency ranges.

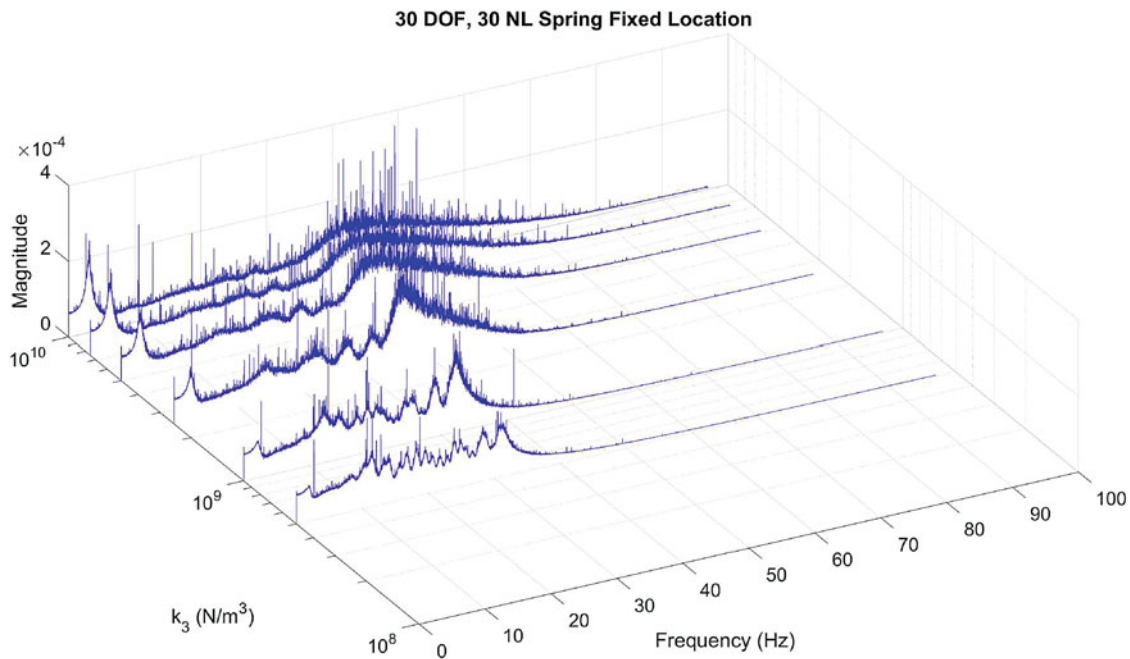


Fig. 45.15 FRF generated in the same manner as Fig. 45.12 investigating $5 \times 10^8 < k_3 < 1 \times 10^{10} \text{ N m}^{-3}$

The hypothesis that increasing the number of nonlinearities in the system would amplify this effect can be supported by the results shown in Figs. 45.13 and 45.14. With increasing numbers of nonlinearities in the system, the degradation of linear modal structure happens to a greater extent and at a lower value of k_3 . There is potentially a simple physical interpretation of the low frequency behaviour seen in the FRF plots; the build up of energy around the first natural frequency of the system is representative of the system stiffening to the point of ‘locking up’ with all the masses moving in phase.

In all three cases the transition, from structure with many clearly visible peaks to a situation where the structure is washed out, occurs in the range $10^8 < k_3 < 10^{10} \text{ N m}^{-3}$. In order to observe the change in a little more detail, simulations were run with a number of k_3 values in this range. The results of these additional runs are shown in Figs. 45.15, 45.16, and 45.17. The closer inspection of the transition away from distinct modal structure shows more clearly the movement of energy towards the ends of the spectrum. The lower frequency modes, except the first, appear to be the first to be washed out by the increasing effect of the nonlinearities.

These plots show more clearly the effect of the increased number of nonlinearities in the system. For the cases with 30 or 50 nonlinearities (Figs. 45.15 and 45.16) more remnants of the linear modal structure can be seen even at very high values for k_3 . In addition to this, the higher frequency peak becomes flatter in the presence of an increased number of nonlinearities. Interestingly, on close inspection, the two surviving peaks at high levels of nonlinearity both show the behaviour of an SdoF Duffing oscillator system using statistical linearisation i.e. with increasing nonlinearity, the peaks shift upward in frequency and down in magnitude.

A number of further simulations were run to confirm that the effects here were genuinely an effect of the increased nonlinearity in the system and not artefacts of the solver or the specific realisations of the nonlinear spring positions. These runs considered different realisations of the random spring positions and showed that the results were insensitive to the realisations as long as many springs were added.

45.4 Conclusions

The results shown in this paper demonstrate that for a system under random excitation with many nonlinear components, when those components are sufficiently excited, the underlying linear modal structure of the system is largely ‘washed out’ by nonlinear effects. Given a sufficient number of nonlinearities this appears to lead to a simplified statistical order in the

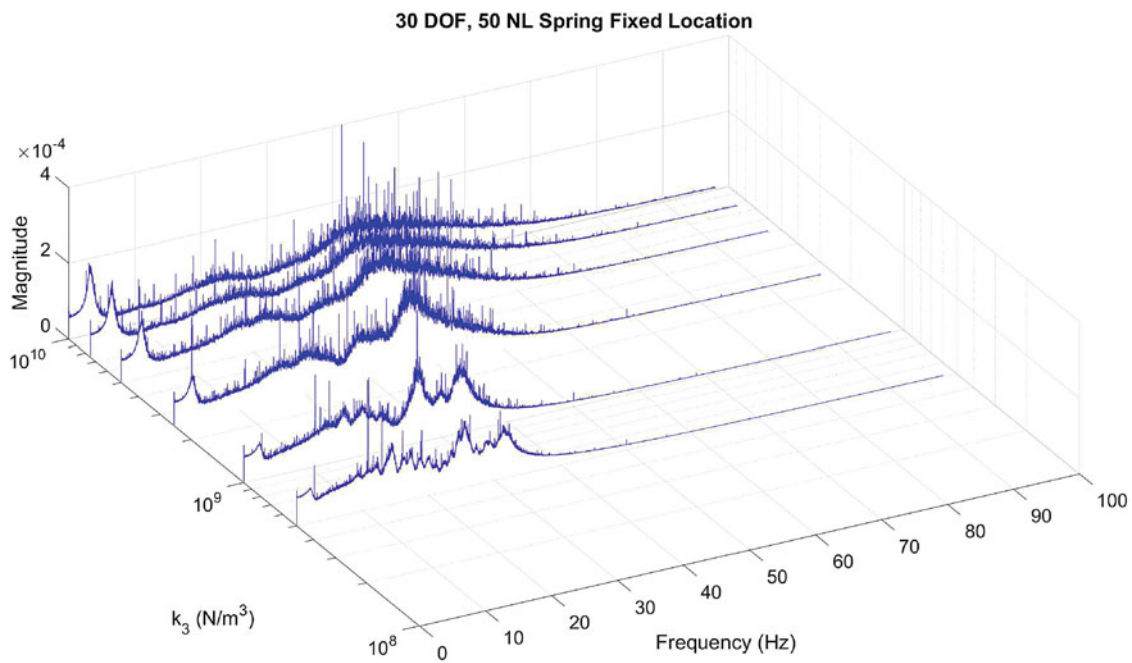


Fig. 45.16 FRF generated in the same manner as Fig. 45.13 investigating $5 \times 10^8 < k_3 < 1 \times 10^{10} \text{ N m}^{-3}$

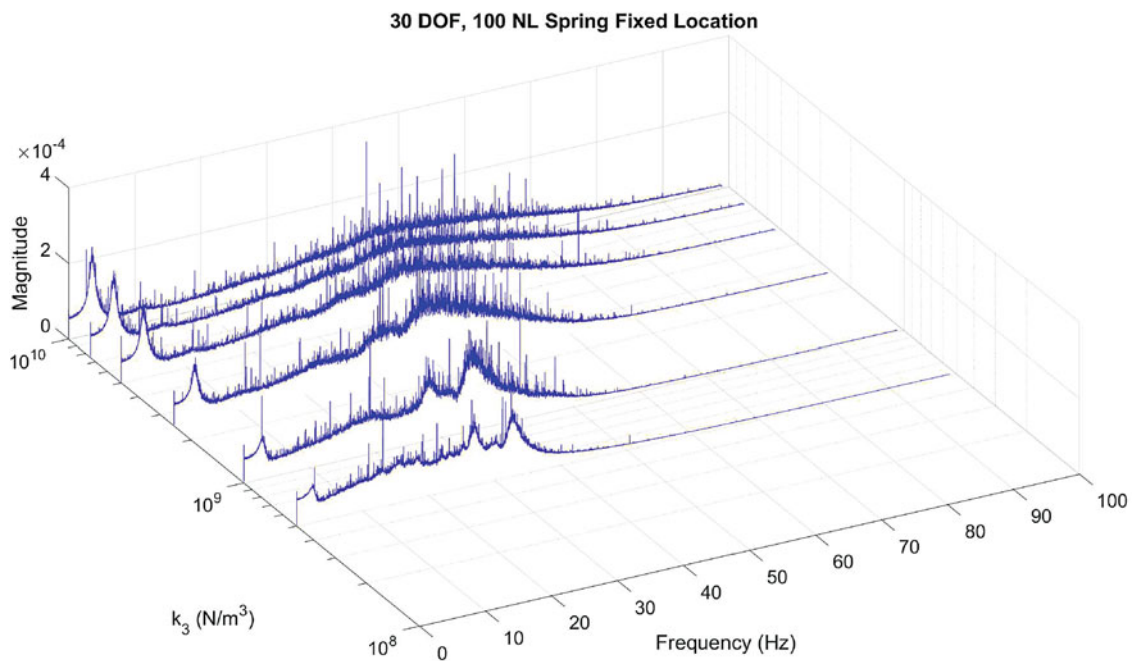


Fig. 45.17 FRF generated in the same manner as Fig. 45.14 investigating $5 \times 10^8 < k_3 < 1 \times 10^{10} \text{ N m}^{-3}$

system from which analogies may potentially be drawn with methods such as SEA. This order emerges more readily with increasing numbers of nonlinearities in the system and the positions of those nonlinearities become less significant as the number increases. It is very clear that this paper has only scratched the surface of this issue and a great deal of further work remains to be done to confirm the results presented here and to begin the process of theoretical explanation.

References

1. Worden, K., Tomlinson, G.R.: *Nonlinearity in Structural Dynamics: Detection, Modelling and Identification*. Institute of Physics Publishing, London (2001)
2. Lanczos, C.: *An Iteration Method for the Solution of the Eigenvalue Problem of Linear Differential and Integral Operators*. United States Government Press Office, Washington, DC (1950)
3. Guyan, R.J.: Reduction of stiffness and mass matrices. *AIAA J.* **3**, 380–380 (1965)
4. Lyon, R.H.: *Statistical Energy Analysis of Dynamical Systems: Theory and Applications*. MIT, Cambridge (1975)
5. Lyon, R.H.: *Theory and Application of Statistical Energy Analysis*. Elsevier, Amsterdam (2014)
6. Spelman, G.M., Langley, R.S.: Statistical energy analysis of nonlinear vibrating systems. *Phil. Trans. R. Soc. A* **2015** 373 20140400; DOI: 10.1098/rsta.2014.0400, **373** (2015)
7. *The Matlab Primer*. The Mathworks (2015)
8. Chapra, S.C., Canale, R.P.: *Numerical Methods for Engineers*, 5th edn. McGraw-Hill, New York (2010)
9. Hickey, D., Worden, K., Platten, M.F., Wright, J.R., Cooper, J.E.: Higher-order spectra for identification of nonlinear modal coupling. *Mech. Syst. Signal Process.* **23**, 1037–1061 (2009)